ISTITUTO NAZIONALE DI FISICA NUCLEARE

Sezione di Trieste

INFN/AE-93/27

21 dicembre 1993

G. Barbiellini, A. Martinis and F. Scuri

A SIMULATION STUDY OF THE BEHAVIOUR OF FINE MESH PHOTOMULTIPLIERS IN MAGNETIC FIELD

Servizio Documentazione
dei Laboratori Nazionali di Frascati

A simulation study of the behaviour of fine mesh photomultipliers in magnetic field

G. Barbiellini[a], A. Martinis[a], F. Scuri[b]

December 13, 1993

Abstract

Results of a Monte Carlo simulation study on fine-mesh photomultipliers (PM) behaviour in magnetic field (B) are reported. This work is accomplished in order to understand the details of the electron cascade between the dynodes: transit time and transit time spread are investigated as well as gain, with respect of several relative orientations of the field and the PM axis for two values of the B-field intensity, 0.14 and 0.28 T, at which some experimental results are also available. Some characteristic of the energy spectrum of the secondary electron emission (SEE) is also taken into account in this work. The aim is to better understand which technical constructive parameters are more sensitive to the optimization of the PM performance in presence of high B-fields (e.g. as required for the KLOE experiment). The simulation results are compared with those experimentally obtained with the Hamamatsu R2490-05 fine mesh tubes.

a: Dip. di Fisica, Università di Trieste and I.N.F.N. sez. di Trieste
b: Dip. di Fisica, Università di Udine and I.N.F.N. sez. di Trieste

1 Introduction

In the context of the KLOE experiment at the DAΦNE ϕ-factory [1, 2] (I.N.F.N. - L.N.F. Frascati) it is compulsory to reconstruct the K_L° vertex in the $K_L^\circ \to \pi^\circ\pi^\circ$ decay with an accuracy of few mm to define the fiducial volume. In particular, for the pattern recognition it is required for the e.m. calorimeter a time measurement resolution of 300 ps and an energy resolution of the order of $5\%/\sqrt{E(GeV)}$. The KLOE e.m. calorimeter is constituted by alternate layers of lead and scintillating fibers and it is read by a certain number of photomultipliers coupled with it by means of plexiglass light guides. The whole detector is confined inside a 6 m diameter solenoid; the magnetic field has a central value of 5000 Gauss and a value of $\sim$ 1000 Gauss at the PM location where the transverse component of the field with respect to the tube axis is about 300 Gauss. The geometrical construction of the calorimeter will be simplified if the PM can operate inside the solenoidal magnetic field. For this reason it was decided to experimentally study the behaviour in magnetic field of parallel mesh PM which use electrodes constituted by a very fine mesh; the electron multiplication and drift take place between the meshes. The dynode effective surface is greater than that of usual phototubes assuring a smaller dependence of the tubes behaviour on the magnetic field.

A special purpose Monte Carlo was written to investigate which construction parameters are more relevant in determining the electron transport and amplification inside the PM's.

Some details of the simulation program are described in section 2; section 3 is devoted to the discussion of the secondary electron emission (S.E.E.) in the multiplication process; in section 4 experimental and simulated data are compared, and some conclusions on the behaviour of the analysed PM' s in magnetic field are summarized in section 5.

2 The Monte Carlo simulation

To understand the timing performances and the sharp cut-off in the experimentally measured gain as a function of the angle ϑ between the tube axis and the magnetic field direction (see below), the process of light signal amplification by multiplication of the electrons in the mesh structure was simulated at the computer also with the aim of looking for possible hints towards an improvement in the devices performances.

Based on the available informations on the construction characteristics, the PM's geometry in the simulation was set as follows: the tubes have cylindrical symmetry with a basis diameter of 2 inches; there are 16 grids (in the following called "dynodes") for the multiplication of the electrons, separated by a distance of 1 mm, while the distance of the photocathode from the first dynode is 2.5 mm. The potential difference between cathode and anode is set to 2500 Volt, but the potential step between cathode and first dynode is twice that between two normal dynodes [3]. Some simplification was introduced in simulating the photomultipliers to compute the value of the Electric field: the mesh structure of the grids (the wire separation is about 11 μm and their diameter 5.5 μm) was approximated by plane square plates of side 36 mm. Actually this assumption affects the shape of the electric field near the grids, but we considered that in a geometry made of wires and holes the real electric field would have guided the electrons towards the wires and

so, for them, apart from a displacement that seems negligible for all practical purposes, everything goes as if they impinged on a solid plate. The edge effects of the electric field were neglected, assuming that it is uniform and constant between the dynodes as in an ideal capacitor. Since we could not trust completely in that, we calculated the exact value of the field and tried to trace some particle trajectory: after a comparison between the results obtained with the approximated field we discovered that all the variables of interest do not differ for more than some percent; to save computation time it was decided to proceed in the approximated way.

The equation of the motion of an electron in electric and magnetic fields was solved and the trajectory for each of particle was traced by points separated by an adequate step in time (see fig. 1). During the passage of the electrons from a mesh to the next one, controls were done on the electron trajectories: in particular, due to the bending effect of the Lorentz force, electrons are considered lost if they hit the walls of the phototube or if they reverse their motion coming back to the mesh that generated them. If none of those cases happens the electron is considered to be safely arrived to the next grid and then it gives rise to the processes of multiplication.

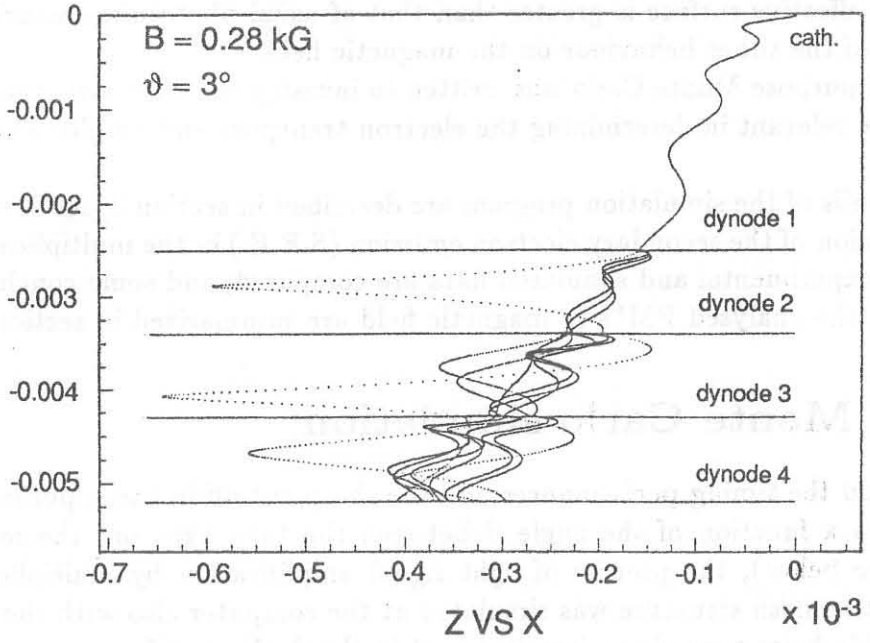

Figure 1: Trajectories of the particles as traced by the computer.

2.1 The multiplication process

The secondary electron emission from solids is a very complicated and complex matter still object of study. In the literature there exist only qualitative plots for what concerns the angular and energy distribution of the secondary electrons yielded from a photon or an energetic primary electron. But, apart from some small difference, the authors consulted [4, 5, 6, 7, 8] are in agreement on what follows:

- the primary electrons (including the primary photoelectrons, i.e. those obtained by a photoionization process) interact at random points in the bulk of the target,

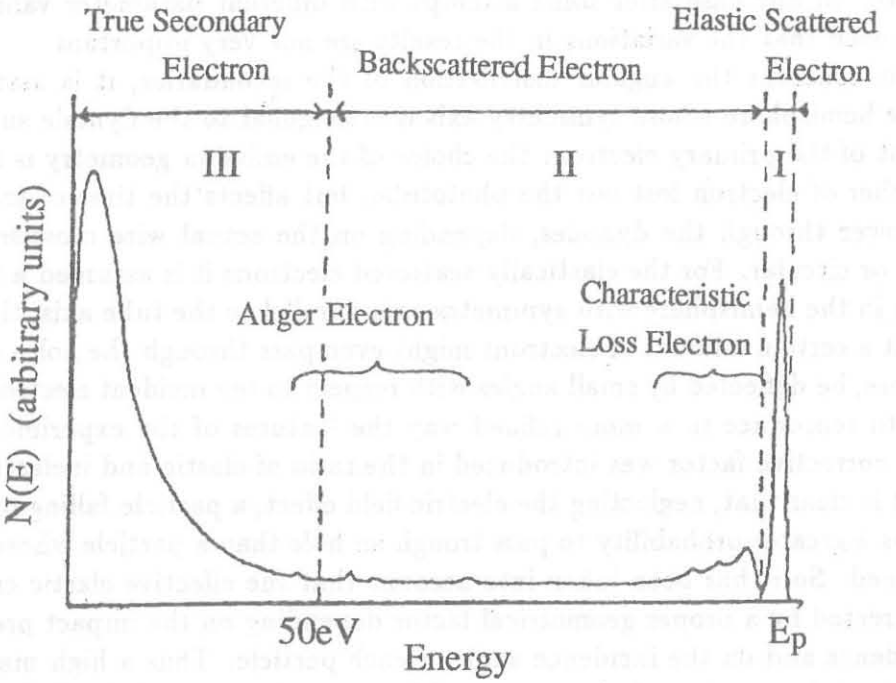

Figure 2: The general shape of the energy distribution of secondary electrons.

- the type of interaction (elastic or inelastic) has to be selected randomly, according to the relative cross sections of the processes,
- the inelastic scattering includes several mechanisms of interaction: ionization, excitation, collective interactions, phonon excitations, etc. ...
- the energies and the angles of deflection of the scattered primary electrons (i.e. most energetic ones) and the ejected secondary electron (low energy ones) are sampled from the cumulative probability distributions.

All these assumptions are model-dependent, so the results are different for different techniques of secondary electron emission (SEE) generation; nevertheless, for the problems afforded here, this is not of dramatic relevance because of the following facts: referring to fig. 2 where the energy distribution of the S.E.E. is plotted for incident electrons of 150 eV, the approximate energy acquired by electrons accelerated between two dynodes, one sees that most of the extracted electrons have an energy below 50 eV (they are the true secondary electrons in region III of the figure). The electrons in region II are relatively few and are the so called "rediffused primaries", that is, electrons that underwent multiple scattering before appearing at the surface of the target. To this group even Auger electrons belong. In region I, that is centered at the energy of the impinging primary electron, there are particles that suffered elastic scattering. The most important parameter is the ratio between the areas of the three regions: the calculation was performed assuming that the electrons in region III are the 80% of the total. The regions I and II are treated in the same way assuming that a truncated gaussian distribution with maximum at the energy of the incident electron has a tail at low energies. It is difficult to be more precise because the informations about the properties of the material the grids are made by, were

not complete. In any case after some attempt with different parameter values, one can convince himself that the variations in the results are not very important.

For what concerns the angular distribution of the secondaries, it is assumed to be flat over the hemisphere whose symmetry axis is orthogonal to the dynode surface at the impact point of the primary electron: the choice of the emission geometry is not influent on the number of electron lost out the phototube, but affects the time of transit of the electron shower through the dynodes, depending on the actual wire cross-section type, rectangular or circular. For the elastically scattered electrons it is assumed a flat angular distribution in the hemisphere with symmetry axis parallel to the tube axis; this accounts the fact that a certain amount of electrons might even pass through the holes of the mesh and, therefore, be deflected by small angles with respect to the incident electron direction.

Finally to reproduce in a more refined way the features of the experimental data a geometrical corrective factor was introduced in the ratio of elastic and inelastic scattered electrons: it is clear that, neglecting the electric field effect, a particle falling orthogonally on a grid has a greater probability to pass trough an hole than a particle whose trajectory is very inclined. So it has been taken into account that the effective elastic cross-section must be corrected by a proper geometrical factor depending on the impact probability at normal incidence and on the incidence angle of each particle. Thus a high magnetic field is expected to enhance the gain up to a certain extent because of the deflection of the particle trajectories; actually this is experimentally observed; moreover we checked that in the simulation the average incidence angle is close to the ϑ angle between electric and magnetic fields as it can be proved by a simple approximated analytical calculation.

The number of secondary electrons emitted by a single primary is assumed to follow Poisson statistics; the mean value μ of the Poisson probability function is calculated for each secondary emission with the following formula:

$$\mu = a \cdot E^{\gamma} \tag{1}$$

where E is the impinging particle energy expressed in eV, $\gamma < 1$ is a material dependent empirical parameter and a is a suitable coefficient determining the absolute gain of the phototube; in the simulation a and γ where considered as free parameters to be tuned on the real data. The time jitter of the secondary electron emission is negligible for this kind of problems, being of the order of 10 fs [9].

3 Results

A DecStation Alpha 3000/300 (Digital Equipment Corporation) was used to run the simulation program and 100 events were generated for each value of the magnetic field and of the angle ϑ between field direction and phototube axis. An event is defined as a photon of energy in the range of green light impinging on the centre of the photocathode. Since the interest is mainly in the response of the tube relative to the emission of a single photoelectron from the cathode, the work is limited to that configuration when running the simulation program, nevertheless a two photoelectrons event sample was generated to check if the output was consistent with what was expected from the experimental histograms relative to the same situation. No particular mechanism of photoemission was studied for the moment, because this work is intended for a deeper understanding of the

ϑ (deg)	*relative gain*						
	B=0.1 T *real*[13]	B=0.13 T *real*[10]	B=0.14 T *real*[11]	B=0.14 T MC	B=0.28 T *real*[11]	B=0.28 T MC	B=0.5 T *real*[13]
0	1.0	1.0	0.7	0.8	0.8	1.0	0.5
10	1.2	1.2	0.9	1.0	0.7	1.1	0.7
20	1.3	1.3	1.0	1.0	1.0	1.2	0.8
30	1.5	1.6	1.0	1.5	1.3	1.4	1.0
40	1.8	2.6	-	1.6	-	1.7	-
50	2.0	3.8	-	1.7	-	2.2	1.2
55	-	-	-	2.1	-	-	-
60	< 0.1	< 0.1	-	< 0.1	-	< 0.1	< 0.1

Table 1: Phototube gain relative to the B=0 T value; real data are associated to the corresponding reference.

electron shower inside the grid structure of the phototube. The electrons emitted by the cathode are given a fixed kinetic energy and a random angle in the downward direction (i.e. towards the anode). It took about 2 hours of c.p.u. time to complete a job.

Two values of the magnetic field, 1400 Gauss and 2800 Gauss, were used to compare the results of the simulation with available experimental data [11]; simulation results are summarized in table 1 and table 2.

In table 1 the angular dependence of the phototube gain relative to the B=0 T condition as obtained from simulation is compared with the available experimental measurements of the same quantity in the 0.1-0.5 T range for the magnetic field. The gain is calculated as the number of electrons collected divided by the number of those emitted by the cathode (only one, in the simulation). A remark must be added: due to the lack of an experimental whole angular scan at different B values, the tuning of the Monte Carlo parameters is not perfect; in figure 3 the effect on the relative gain curve shape is shown, when varying in the range $0.45 - 0.55$ the empirical parameter γ defined above. Nevertheless, from figure 4 a good agreement between real and simulated data in the gain curves is evident for $\gamma = 0.45$

In figure 5 the electron transit time curve as a function of the angle ϑ is plotted for real and simulated data at $B = 1400$ Gauss and $B = 2800$ Gauss; some remark must be taken into account for a proper comparison of the curves:

- The transit time is calculated as the average of the distribution of the mean arrival times on the anode in each event. This last quantity is close to the peak value of the arrival time distribution (see fig. 6 a)); the arrival time is defined as the elapsed time from the photoemission and the electron arrival on the anode.

- the absolute value of the transit time in the real data is measured with respect to a time base signal defined by the trigger and not with respect to the photoelectron emission as in the Monte Carlo; nevertheless the shape of the curve is well reproduced by the simulation.

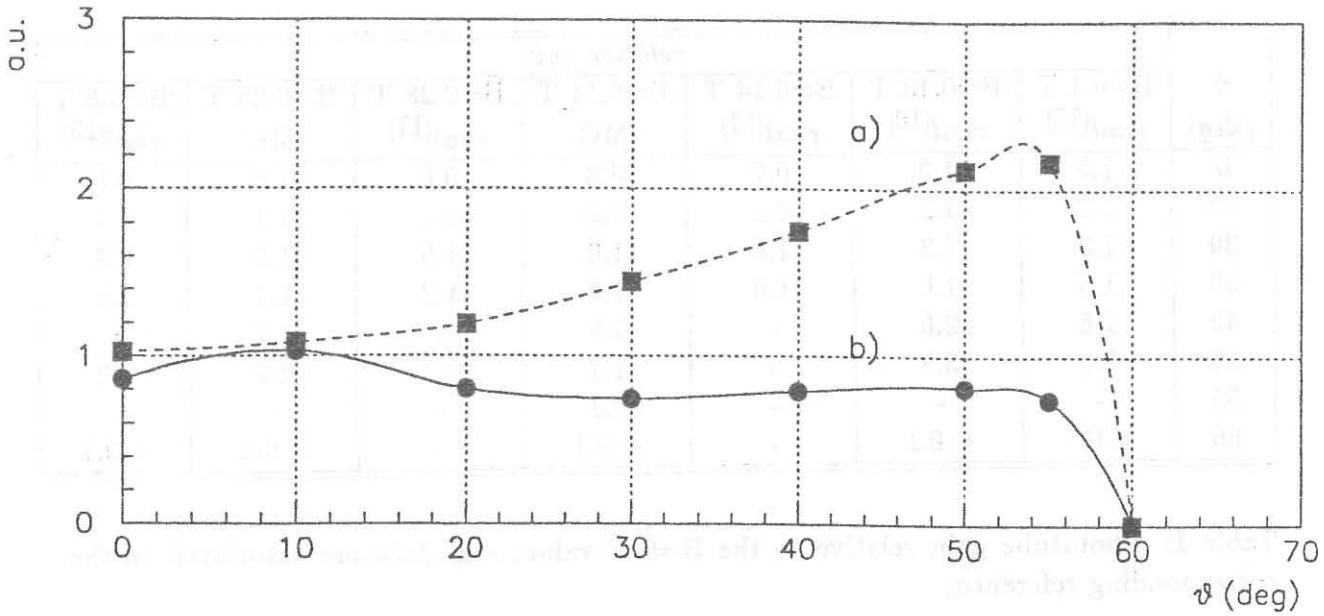

Figure 3: Relative gain at 2800 Gauss for two values of the parameters a and γ of formula (1); a) $a = 0.2$, $\gamma = 0.45$ and b) $a = 0.1$, $\gamma = 0.55$

In table 2 real and simulated data are summarized for the transit time spread (t.t.s.) measurements; the t.t.s. is defined as the FWHM of the distribution of the mean transit times (fig. 6 b)). For a proper comparison between real and simulated data one must consider that in the real data the t.t.s.results in a convolution of the spread in the calorimeter fiber light emission and transport and of the proper PM time spread in photoemission and electron transport; moreover, real data refer to events with about 40 photoelectrons in average.

From the previous analysis it's clear that the simulation well describes the gross features of the PM; apart different normalization factors whose origin is described above, the shape of the curves is equal in simulated and real data for gain, average transit time, and t.t.s. as a function of the angle ϑ. Moreover, in the simulated data the absolute value of the average transit time and of the t.t.s. are well compatible with the upper limits

	transit time spread			
ϑ	$B = 0.14T$		$B = 0.28T$	
(deg)	real	MC	real	MC
0	350	280 ± 30	340	250 ± 30
10	380	220 ± 30	340	240 ± 30
20	350	260 ± 30	330	260 ± 30
30	350	250 ± 30	340	200 ± 30
40	-	260 ± 30	-	220 ± 30
50	-	200 ± 30	-	200 ± 30

Table 2: Transit time spread; real data are taken from ref.[11].

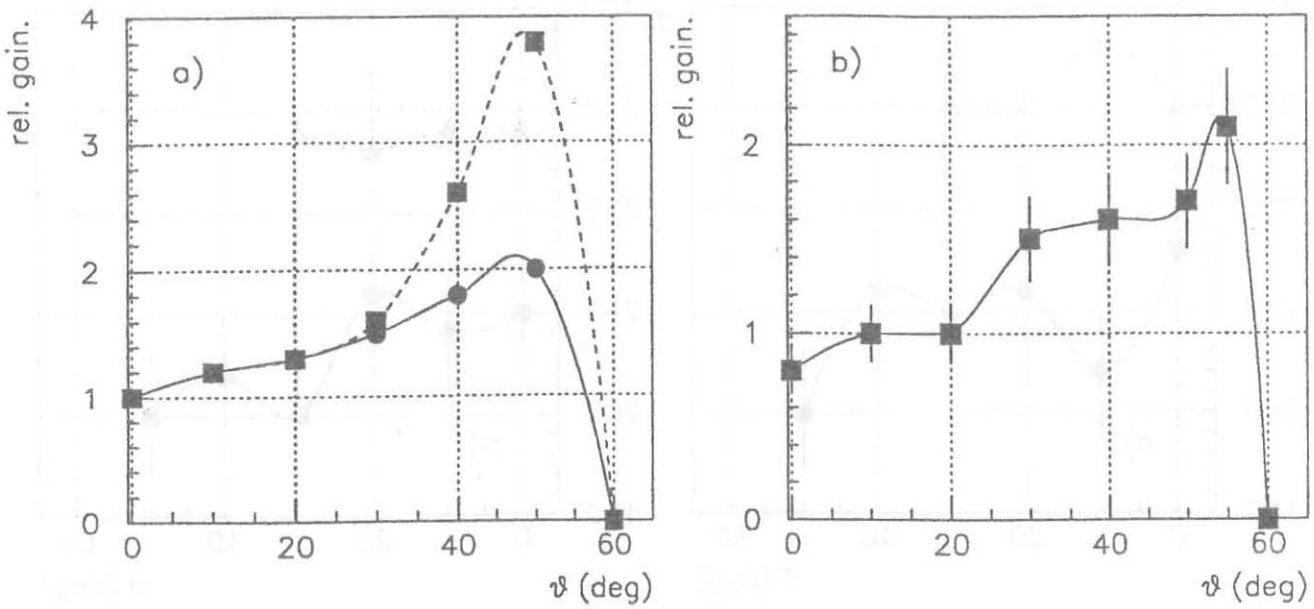

Figure 4: Relative gain at 1400 Gauss; a) real data, ref. [10] and ref. [13]; b) simulated data.

quoted by the firm [12] and in good agreement with the one photoelectron available measurements for t.t.s. [13]. For these reasons, results of the Monte Carlo were considered reliable and the simulation was fully exploited for a deeper analysis of the dependence of the PM main features on the constructive parameters by separately varying the free parameters of the simulation; the results of this particular study can be summarized as follows:

- the most relevant effects on the gain, transit time and t.t.s. are given by the combined variation of the parameters μ and γ in formula (1); depending on the effective impact probability on the grid of the impinging electron electrons, the multiplication can be mainly determined or not by those electrons that cross a mesh without strong interaction on wires and arrive with twice kinetic energy on the next grid;

- the t.t.s. performance is mainly determined by the grid geometry; since the impinging electron excites a number of secondaries that get off the metal surface with a direction distributed around the normal to the surface, in the case of rectangular wire cross-section emission towards the cathode is more favoured than in the case of circular cross-section (fig. 7); the transit time spread increases by a 50% when changing form the former case to the second in the simulation; moreover, especially at high magnetic field values, the emitted particle has a greater probability of falling on the emitting when spiralizing with a little curvature radius;

- the S.E.E. average energy, a material dependent parameter, slightly affects only the t.t.s.; by comparing results obtained with $3.5eV$ and $20eV$ for the average energy of the true secondaries, an increase of lower than 20% in t.t.s was seen at higher energy due to the corresponding greater spread in velocity for the emitted particles.

- The mesh density in the grid must be optimized as a function of the PM gain;

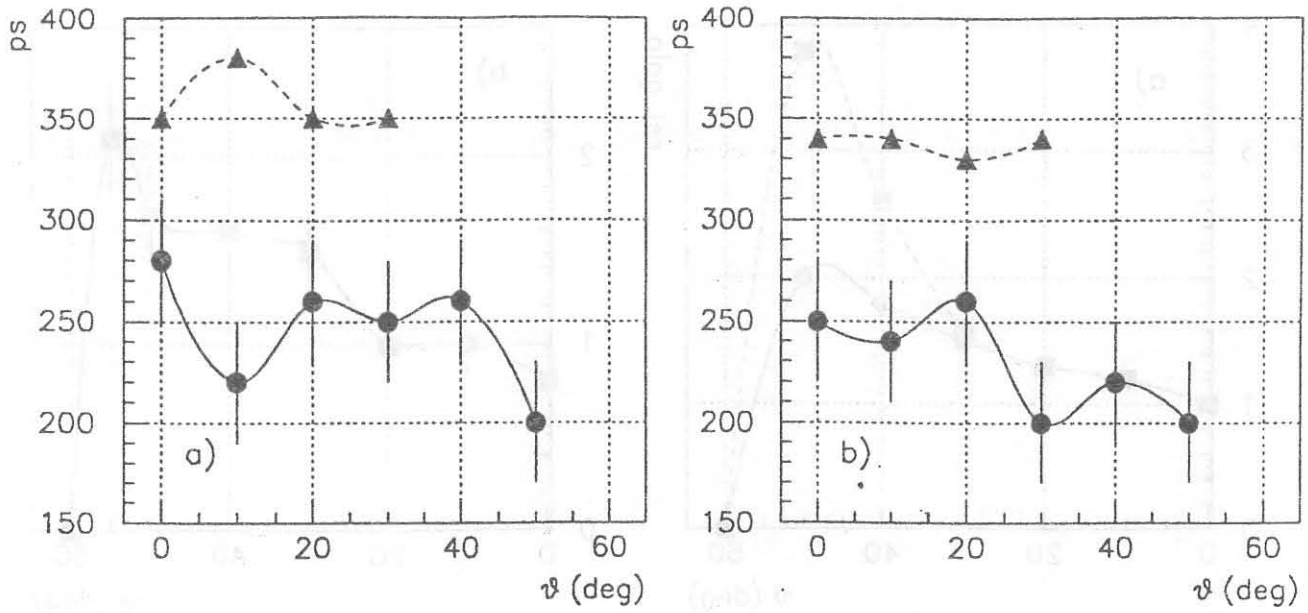

Figure 5: Transit time curves; triangles: real data; circles: simulated data; a) $B = 1400$ Gauss, b) $B = 2800$ Gauss.

from the impact probability study it comes out that a best compromise must be found between the need of a high impact probability for electrons accelerated in between two grids and the need of a low impact probability for low energy backwards extracted electrons; in the simulation, studies were performed by varying the impact probability at normal incidence around 50%, the actual fraction of the wire area over the grid surface.

Finally, a relevant remark must be added to complete the discussion; the sharp cut-off in the gain curve above $\vartheta = 55^o$ is mainly determined by the lost of the electron cloud on the PM wall in the last amplification stage, due to the drift velocity of charges in crossed magnetic and electric fields. This gives an additional hint for a constructive constraint: the smaller is the radius of the photomultiplier structure, the lower is the dynode number useful for amplification at fixed voltage difference between grids.

It has to be noted also that the transit time is greater for greater angles, but it seems to be independent from the field value. The transit time spread, otherwise, seems to be almost constant within the errors regardless to the field and angle values.

4 Conclusions

From the results presented in the previous sections it appears clear that the simulation well reproduces the gross features of the PM behaviour in magnetic field: in particular the gain increasing, up to a certain B-field angle is well reproduced and the sharp cut-

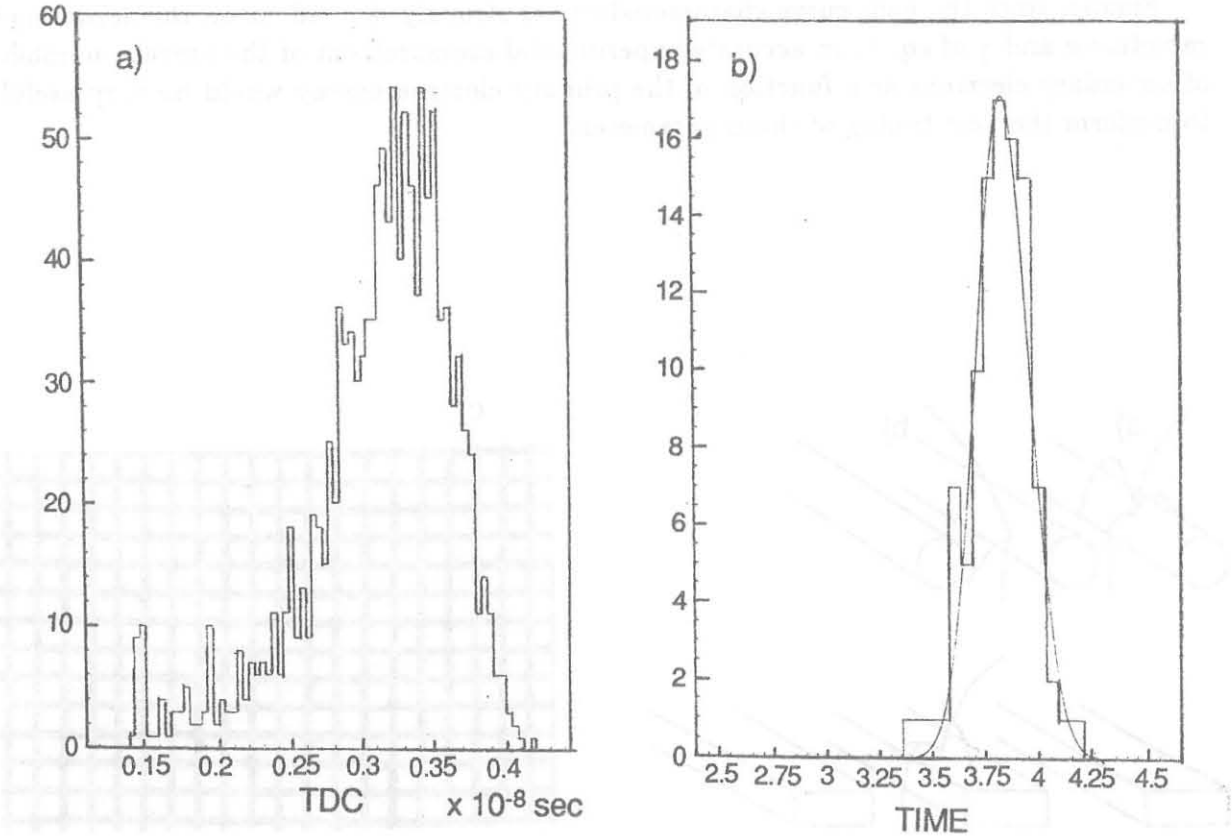

Figure 6: a) Typical electron arrival time distribution for a single event, b) Mean arrival time distribution

off appears at a reasonable angle so that for what concerns the gain there is a good agreement with experimental data (however in the simulation the gain was kept lower for computation time problems). The only cause of electron losses is represented by the fact that the particles are deflected by an angle that is on average the same of that of B-field relative to the PM axis; so for large angles the electrons fall out the grids surface and are lost. This suggests that a PM with bigger diameter should suffer less the effects of the magnetic field. Alternatively one has to reduce the length of the PM itself by reducing the number of multiplication stages (but the gain is also lowered) or by putting the dynodes nearer to each other (paying attention to the value of the E-field between the grids).

Even the t.t. and t.t.s. follow the expected behaviour. From an accurate study it comes out also that the correlation between the mesh structure ("round wire" or "rectangular wire") and the trajectory of the emitted electrons actually affects mainly the transit time spread. T.t. and t.t.s. are also sensitive to the shape of the energy distribution function: in particular in the more realistic situation where the electrons are mainly back-scattered, low values of the peak and r.m.s. of true secondaries imply low transit time and transit time spread values.

Finally, since the gain curve characteristics are strongly dependent on the actual parameters a and γ of eq. 1, an accurate experimental measurement of the average number of secondary electrons as a function of the primary electron energy would be very useful to perform the best tuning of those parameters.

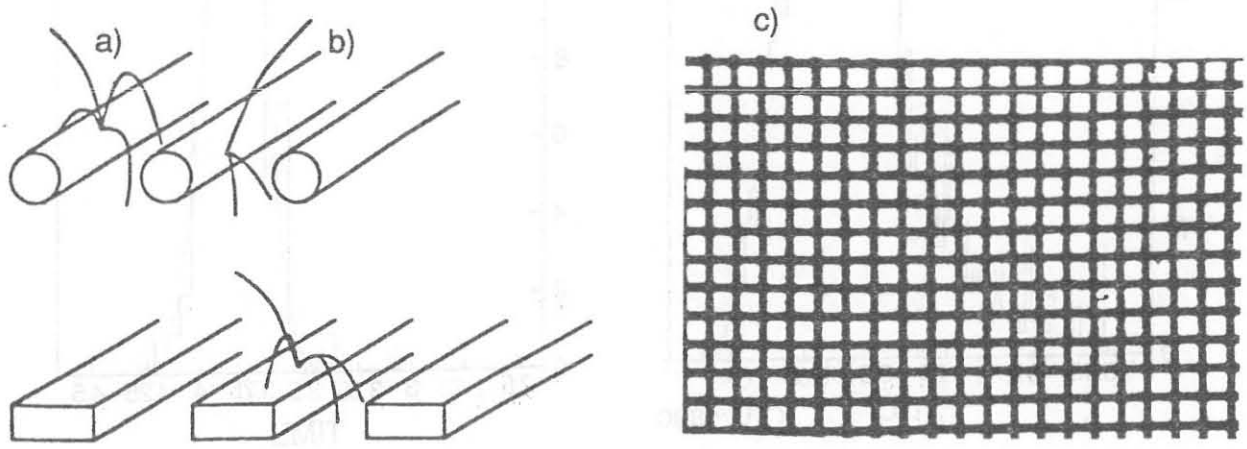

Figure 7: Possible cross-section of the grid wires: for the circular section case there can be a) backward and b) forward emission; in the rectangular case only backward emission is favoured and not all the secondary electrons pass through the mesh. c) microscope photographic picture of a real grid: 11 μm wire separation, 5.5 μm wire size.

References

[1] A. Aloisio et al. (KLOE collaboration): *KLOE, a general purpose detector for DAΦNE* LNF-92/019 (IR) April, 1 1992

[2] C. Bloise, Proceedings of the Workshop on Physics and Detectors for Daphne. G. Pancheri Ed., Frascati, 1991.

[3] R. Enomoto et al., Feasibility Study of Single-Photon Counting Using a Fine-mesh Phototube for an Aerogel Readout. KEK preprint 93-3 April 1993 H (To be published in N.I.M., A).

[4] O. Hachenberg and W. Brauer, Secondary Electron Emission from Solids. Adv. Electronics and Electron Physics 11,413-499 (1959)

[5] A. Akkerman et al., Secondary electron emission from alkali halides induced by X-rays and electrons. WIS-92/57/jul-PH

[6] D. Briggs, J. C. Rivière, Practical Surface Analysis by Auger and X-ray Photoelectron Spectroscopy (chapter 3). Edited by D. Briggs and M. P. Seah. ©1993, John Wiley & Sons, Ltd.

[7] R. Feder, Polarized electrons in surface physics (chapter 4). World Scientific

[8] A. Modinos, Field, Thermionic and Secondary Electron Emission Spectroscopy. Plenum N.Y.

[9] Hamamatsu Photonics Italia: private communication.

[10] C.Bini et al., Gain and photoelectron number dependence on the angle around the axis for Hamamatsu R3423-01 and R2490-05 photomultipliers in a magnetic field, Kloe note 50/1993, February 23, 1993.

[11] M. Anelli et al., Beam test of Hamamatsu R2490-05 tube in a 2.8 KGauss magnetic field, Kloe note 60/1993, June 10, 1993.

[12] Hamamatsu Photonics, Photomultiplier Tubes and Asemblies Catalog, August 1993, page 27.

[13] Timing Characteristics of Micro-Channel Plate and Fine Mesh Photomultiplier Tubes in a 1 Tesla Field. KEK Preprint 92-57 July 1992 H.